International Journal of Engineering

Journal Homepage: www.ije.ir

Design and Analysis of High Efficiency Perovskite Solar Cells with Light Trapping Nano-textured Substrates

H. Abedini-Ahangarkola, S. Soleimani-Amiri*

Department of Electrical and Computer Engineering, Babol Noshirvani University of Technology, Babol, Iran

PAPER INFO

Paper history:
Received 01 September 2020
Received in revised form 09 November 2020
Accepted 09 January 2021

Keywords:
Perovskite Solar Cells
Nano-textured
COMSOL Multiphysics
Finite Element Method

ABSTRACT

Recently, the utilization of hybrid organic-inorganic perovskite solar cells under advanced light management designs have attracted intensive attention. In this study, a three-dimensional (3D) finite element method (FEM) technique was used in the COMSOL Multiphysics simulation package to investigate coupled optical and electrical characteristics of perovskite solar cells (PSCs) with light trapping nanostructures. Upon the use of nano-textured fluorine-doped tin oxide (FTO) substrates, we propose two architectures which can guide and trap the light at nanometer dimensions. Two proposed PSCs i.e. concave and trapezoidal structures are compared to the planar structure in order to investigate the effects of using nanostructured substrates on the optoelectronic performance of PSCs. Optical analysis reveals that using optimized concave and trapezoidal structures can enhance the light absorption up to 32 and 26%, respectively at the wavelength of 550 nm. Electrical simulations have shown that in addition to enhanced total carrier generation, the generated carriers can be effectively collected in the proposed nanostructured PSCs. Accordingly, the short-circuit current has risen from 20 mA for planar structure to 25.7 mA for concave and 23.2 mA for trapezoidal PSCs. After analyzing various heights and adopting optimum values, the power conversion efficiency for concave and trapezoidal PSCs experienced substantial increase of 5.5 and 3.5%, compared to the planar structure. These drastic improvements analyzed by coupled optical and electrical modelling of nanostructures can pave the way for further studies to fabricate high efficiency PSCs with nano-textured substrates as a light-trapping technique.

***doi**: 10.5829/ije.2021.34.04a.13*

1. INTRODUCTION

Hybrid halide perovskite has attracted so much attention as a great photoactive material in photovoltaic device applications due to its large absorption coefficient [1, 2], an appropriate and tunable band gap [3], long carrier diffusion length and fabulous efficiency in harvesting energy [4]. Moreover, the simplicity of manufacturing process and the feasibility of being integrated with traditional photovoltaics such as Si and CIGS to build efficient tandem devices are some of the other advantages of perovskite solar cells (PSCs) which would surely outweigh their disadvantages, such as vulnerability due to exposure to moisture, heat, etc [5, 6]. In the course of the years 2009 to 2016, the efficiency of PSCs increased from 3.8 to above 22% [7-9]. The optimization of perovskite preparation and deposition methods, the enhancement of interface quality and degradation mitigation are the main approaches that have been used in the ongoing efforts to achieve PSCs with a greater efficiency. Besides, different device configurations were developed, including the original mesoporous n-i-p junction and mesoporous-free planar junction with regular (n-i-p) and inverted structure (p-i-n) [10, 11].

Although tremendous progress has been made, many challenges for PSCs still exist. The most important problem is the conflict between the amount of carrier photo-generation and collection. As we all know, the thickness of the perovskite layer should be less than the diffusion length of carriers for efficient extraction, whereas the thin perovskite material will lead to insufficient light absorption, which means fewer

*Corresponding Author Institutional Email: *s.soleimani@nit.ac.ir* (S. Soleimani Amiri)

Please cite this article as: H. Abedini Ahangarkola, S. Soleimani Amiri, Design and Analysis of High Efficiency Perovskite Solar Cells with Light Trapping Nano-textured Substrates, International Journal of Engineering, Transactions A: Basics Vol. 34, No. 04, (2021) 873-880

generated carriers [12]. To solve the problem, thin absorbing layers in combination with light trapping techniques are exploited to increase light absorption within the active layer [13].

Generally, there are two typical techniques to enhance optical trapping capability. The first one is the light scattering by increasing the optical paths of the incident light, and the other one is to enhance the surface plasmon resonance effect [14, 15]. Efficient light trapping methods can also lead to decreased manufacturing time and cost. Therefore, acquiring more knowledge to realize light trapping effects in photo absorber layer is necessary for the future development of highly-efficient, environmentally friendly, and low-cost thin film solar cells. It is worth noting that the optical and electrical benefits of light trapping can vary for solar cells different materials. A wide variety of plasmonic and nanophotonic structures were proposed for the first and second generations of solar cells, and many theoretical analyses were carried out to model both electrical and optical behavior in these advanced photovoltaic devices to predict the performance and optimize the structure [16].

In the field of perovskite solar cell, however, studies are relatively limited about various light trapping techniques with experimentally realistic structures and their optical and electrical effects [17, 18]. Abdelraouf et al. [17] used nanotubes, nanorods, nanocones, and nanopyramids as hole transport nanostructures for light trapping and enhancing the PSC performance. They found that the nanotubular structures, which can be fabricated by free standing TiO_2 array, have the highest short circuit current (24.29 mA/cm^2) and overall efficiency (15.23%) among the different investigated nanostructures. Zandi et al. [18] explored the use of corrugated anti and back reflector layers instead of flat ones to improve the power conversion efficiency of PSCs, and demonstrated that in this way they can increase the PCE of their PSC to 17.5%.

In this context, we make an effort to improve the performance of $CH_3NH_3PbI_3$ PSCs using two different sets of nano-textured FTO substrates (periodic concave and trapezoidal structures) as a light trapping method. For each model, using Finite-Element-Method (FEM), we investigate the impact of nanostructures on the light trapping and carrier generation, and then couple the results with electrical model to calculate the short circuit current density (J_{sc}), open circuit voltage (V_{oc}), power conversion efficiency (PCE) and other important characteristics such as incident photon-to-electron conversion efficiency (IPCE). By changing the height, the optimum value of each nanostructure is chosen to demonstrate the superior function of the device and provide a guideline for further research on designing such delicate nano-textured substrates and make the most of light trapping effect.

2. MODELING DETAILS

Our base materials for this simulation work are Au, Spiro-MeOTAD, $CH_3NH_3PbI_3$, TiO_2, FTO and air. It is obvious that fluorine-doped tin oxide (FTO) acts as the transparent conducting oxide (TCO), TiO_2 as the electron transporter layer (ETL), Spiro-MeOTAD as the hole transport layer (HTL) and Au as contact.

The numerical optoelectronic simulations based on finite-element method (FEM) are carried out in COMSOL Multiphysics package. The FEM is a numerical method to calculate boundary condition problems for partial differential equations [18]. In this method, the whole structure is subdivided into small parts by mesh generation, and the equations are solved approximately for each element. For a combined optical-electrical simulation, first we use wave optic module to calculate optical absorption and generation profiles of electrons within the device. In fact, in this step, the Helmholtz equation derived from Maxwell's equation in the frequency domain are solved for each element to obtain optical intensity and photogeneration rate. The equation is given as:

$$\nabla \times (\nabla \times \mathrm{E}) - k_0^2\, \varepsilon_r\, E = 0$$
$$\varepsilon_r(\lambda) = (n(\lambda) - ik(\lambda))^2 , \quad (1)$$

where E is electric field, k is wave-vector and is relative permittivity $\varepsilon_r$which is a function of wavelength. Relative permittivity for each layer is calculated by real part (n) and imaginary part (k) of refractive index extracted from [19-21] and implemented in COMSOL Multiphysics using interpolation function. Standard AM1.5G plane wave source is located above the air and is used as the input power. The wavelength range in our simulation is 300-800 nm with 10 nm resolution. In order to reduce the simulation time, we model a small unit of solar cell with periodic boundary condition (PBC) on the sides of all PSC layers. Only for the Au contact, we define the layer as a perfect electric conductor (PEC).

Setting this condition, the gold acts as a back reflector and most of the unabsorbed photons of the incident light are reflected back to the structure. Using Equation (1), the electric field E can be obtained for the whole domain. Photo generation rate for each wavelength under AM1.5G irradiation can be calculated by (Equation (2)) [18]:

$$G_{opt}(\lambda) = \frac{\varepsilon'' |E|^2}{2\hbar} , \quad (2)$$

where $\hbar$ is the plank constant and ε'' is the imaginary part of the permittivity. As stated before, complex refractive indices and relative permittivity of all layers are taken from previously measured data [18, 22]. By integration of $G_{opt}(\lambda)$ over the wavelength range, the total generation rate (G_{tot}) for the whole spectrum (300-800 nm) is calculated as follows:

$$G_{tot} = \int_{300}^{800} G_{opt}(\lambda)\ d\lambda \quad (3)$$

Then, the calculated total generation rate is used as an input of the semiconductor module to investigate electrical properties of the PSC. By solving Poisson (Equation (4)) and continuity equations (Equations (5), (6)) at each mesh element in semiconductor module the carrier concentration in the structure is obtained

$$\nabla^2\varphi = \frac{\rho}{\varepsilon_0\varepsilon_r} = \frac{q(p+N_D-n-N_A)}{\varepsilon_0\varepsilon_r} \quad (4)$$

$$\frac{\partial n}{\partial t} = \frac{1}{q}\nabla\cdot J_n + G_n - R_n \quad (5)$$

$$\frac{\partial p}{\partial t} = -\frac{1}{q}\nabla\cdot J_p + G_p - R_p \quad (6)$$

where φ is the electrostatic potential, ρ is the total charge density, ε_0 is the permittivity of free space, ε_r is the relative permittivity of semiconductor, q is the electric charge, p and n are the number of charge carriers, N_D and N_A are the concentrations of donor and acceptor impurities, G_n and G_p are the generation rates, and R_n and R_p are the recombination rates of electrons and holes, respectively. As stated before, generation rates $G_n = G_p = G_{tot}$ are imported from the wave optic module results (Equation (2)) to couple optical and electrical models. J_n and J_p are the electron and hole current density, expressed by the electron and hole drift-diffusion charge transport equations as follows:

$$J_n = qn\mu_n E + qD_n\nabla n \quad (7)$$

$$J_p = qp\mu_p E - qD_p\nabla p \quad (8)$$

where μ_n and μ_p are the electron and hole mobility, and D_n and D_p are the electron and hole diffusion coefficient, respectively.

The physical parameters of TiO_2, $CH_3NH_3PbI_3$ and Spiro-MeOTAD used in the semiconductor module are summarized in Table 1 [14, 18]. Shockley-Read-Hall (SRH) recombination, as the dominant recombination mechanism, is taken into consideration in our simulations. The FTO transparent contact and Au back reflector contact are assumed Ohmic ($10\frac{\Omega}{cm^2}$) and Schottky, respectively.

After obtaining the current density-voltage (J-V) characteristics of the solar cell, we can determine fill-factor (FF) and power conversion efficiency (PCE). The fill factor of the device is defined as:

$$FF = \left(J_m \cdot V_m\right)\Big/\left(J_{sc} \cdot V_{oc}\right) \quad (9)$$

where J_m and V_m are the current density and voltage at the maximum power point (P_m), and J_{sc} is short-circuit current density and V_{oc} is open-circuit voltage. Finally, the power conversion efficiency of the solar cell is the proportion of the maximum power output to the input power (P_{in}) according to:

$$\eta = \frac{P_m}{P_{in}} = \frac{(FF \cdot J_{sc} \cdot V_{oc})}{P_{in}} \quad (10)$$

TABLE 1. The electrical parameters of the simulated PSC

Parameter	TiO_2	CH3NH3PbI3	Spiro-OMeTAD
Thickness (nm)	100	300	350
Eg (eV)	3.2	1.55	3.0
$\chi(eV)$	4.0	3.92	3.67
N_C (cm^{-3})	1×10^{19}	1×10^{19}	2×10^{19}
N_V (cm^{-3})	1×10^{19}	1×10^{17}	1×10^{19}
N_D (cm^{-3})	2×10^{18}	-	-
N_A (cm^{-3})	-	3×10^{15}	1×10^{18}
τ_n/τ_p (ns)	5/2	8/8	2/5

3. RESULTS AND DISCUSSION

Figure 1 depicts three-dimensional schematic views of perovskite solar cells with three different geometries used in our simulations. As illustrated in Figure 1(a), the simulated planar n-i-p PSC has a width of 250 nm and a

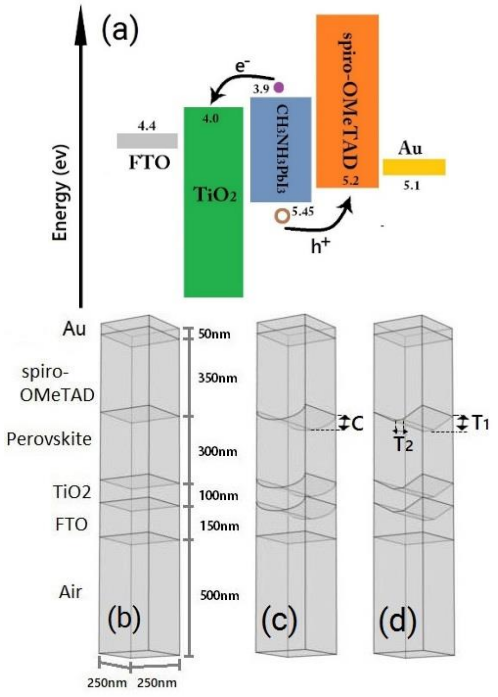

Figure 1. (a) Energy band diagram of the device. Schematic of the simulated PSC with (b) planar (reference cell) (c) concave and (d) trapezoidal structures. All simulated cells have the same dimensions

depth of 250 nm. The structure consists of Air (500 nm thick), FTO substrate (150 nm), TiO_2 as an ETL (100 nm), $CH_3NH_3PbI_3$ as an absorber layer (300 nm), Spiro-OMeTAD as a HTL (350 nm), and Au contact (50 nm). Figures 1(b) and (c) show the cells with the same dimensions on the nano-textured FTO substrates with the concave and trapezoidal groove shapes, respectively. In the concave architecture (Figure 1(b)), the concavity height is denoted by C and in the trapezoidal structure (Figure 1(c)) the height and the short base are denoted by T_1 and T_2, respectively. The energy band diagram of the device (Figure 1(d)) illustrates how photo-generated electrons and holes in the proposed designs are transported to contacts by TiO_2 and Spiro-OMeTAD as ETL and HTL, respectively.

First, to validate the correctness of our constructed model and selection of parameter values in our simulations (Table 1), we try to model and reproduce the experimentally obtained J-V characteristics of the experimental work from Barrit et al. [23] for planar structure (Figure 2).

After achieving a good agreement between the experimental and simulation results of the planar structure, we investigated the effects of using the proposed concave and trapezoidal-shaped FTO substrates on the performance of the PSCs. In order to achieve the optimum value for nanostructures, the height of the concave (C) and trapezoidal structures (T_1) are altered ranging from 40 nm to 70 nm. Meanwhile, the volume of the absorber layer and the thickness of the whole structure are kept unchanged. To clarify the effect of nanostructures shape and size on the absorption of the active layer we define the normalized absorption spectrum as follows:

$$\text{Normalized Absorption}(\lambda) = \frac{\text{Absorption of nanotextured substrate}(\lambda)}{\text{Absorption of planar substrate}(\lambda)}$$

The light absorption of planar structure (with and without Au) over the wavelength range of 300-800 nm is displayed in Figure 3(a), and the normalized absorption spectra in the absorber layer of the concave and trapezoidal structures to their planar counterpart with different sizes are depicted in Figures 3(b-d). As can be seen in Figure 3(b), the maximum absorption improvement reaches around 32% at the wavelength of 560 nm. Although the best enhancement belongs to 70 nm concavity (C=70), the changes of absorption spectra with the height of concavity in most wavelengths are relatively small. Figure 3(c) shows the normalized absorption spectra of trapezoidal architecture with height (T_1) changing from 40 to 70 nm and constant short base of 50 nm (T_2=50 nm), results in a maximum absorption enhancement of 26% at a wavelength of 550 nm. Again, the changes of absorption spectra with trapezoidal groove height is negligible and it can be said that the absorption spectrum is almost independent of the nanostructures height. Figure 3(d) illustrates the normalized absorption spectra of trapezoidal architecture with a short base (T_2) starting from 40 nm to 100 nm, while the height is fixed at 50 nm (T_1=50 nm). It shows that the maximum absorption enhancement of 24% occurs at the wavelength of 380 nm for T_2=60 nm. In the wavelength range of 400-500 nm, we observe absorption increment for the case of trapezoidal structure with T_2=100 nm. To sum up, by integration of absorption values over the wavelength range of 300-800 nm, it can be said that upon using concave and trapezoidal structures with appropriate size the total absorption can be significantly enhanced compared to the planar structure.

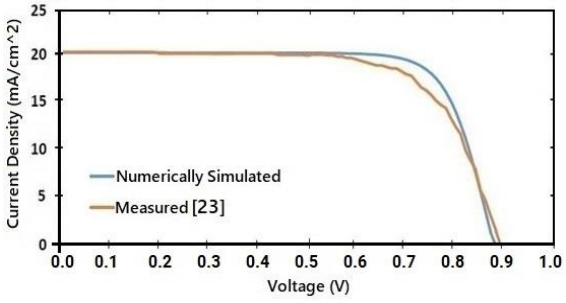

Figure 2. Comparison between the J-V characteristics of experimentally measured and numerically simulated planar perovskite solar cells

Figure 4 illustrates the calculated carrier photo generation rate three-dimensional profiles (Equation (2)) at three different wavelengths of 300, 550 and 800 nm for planar, concave and trapezoidal solar cells. At λ=300 nm, most incident photons with high energy generate electron-hole pairs in TiO_2 and only a few photons can reach the front parts of perovskite and cause weak carrier photo-generation. Trapping of the light between nanostructures in active layer at this wavelength doesn't happen seriously since the most part of the light is absorbed at the ETL and couldn't reach the perovskite layer. At λ=550 nm (Figure 4(b)), however, the photons with lower energy cannot generate any carriers in TiO_2 due to its large bandgap.

Thus, we observe photo-generation of carriers only in $CH_3NH_3PbI_3$ layer especially in its front part near the ETL interface. The significant enhancement of the generation rate in the active layer of concave and trapezoidal structure in comparison with planar structure can be attributed to the light scattering mechanism occurs between the nanostructures wall. The result is in consistent with the normalized absorption spectra peaks (Figures 3(b) and (c)) around 550 nm. Finally, at λ=800 nm (Figure 4(c)) low-energy photons (1.5 eV) can penetrate to all layers of the cell, reach the gold contact and reflect back to the structure. This is related to the lower absorption coefficient of the absorber layer at such

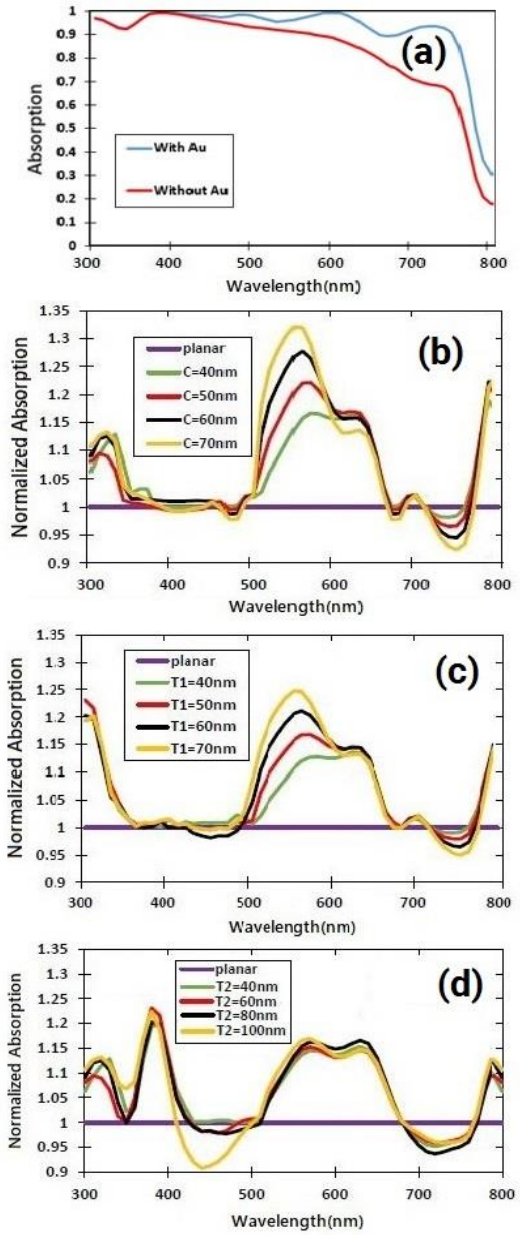

Figure 3. (a) Absorption spectrum of planar structure with and without Au contact layer. Normalized light absorption spectrum in the active area of the (b) concave (c) trapezoidal solar cells with changing the height of the nanostructures. (d) The same spectra for the trapezoidal solar cell with changing the short base size.

high wavelengths. As can be seen in this wavelength, maximum G_{opt} occurs at the middle parts of $CH_3NH_3PbI_3$ layer and also near the interface of HTL due to the reflection and scattering of the light in the structure.

As explained before, by integration of $G_{opt}(\lambda)$ over the wavelength range of 300-800 nm, the total generation rate (G_{tot}) can be calculated (Equation (3)). Then, the obtained total charge density is used as the input of the semiconductor module to probe into electrical properties

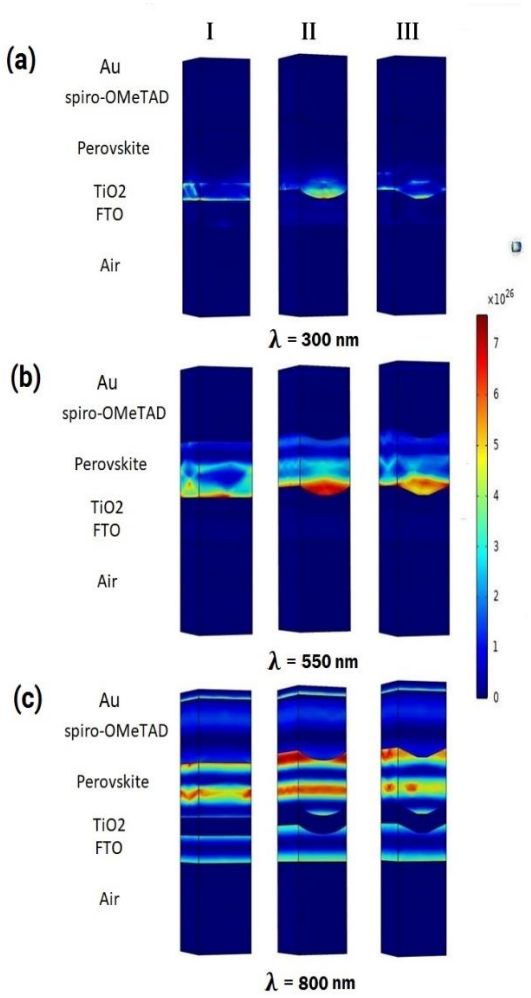

Figure 4. The calculated carrier photo-generation rate profiles ($G_{opt}(\lambda)$) for planar(I), concave (II) and trapezoidal (III) structures at three different incident wavelengths (a) 300 nm (b) 550 nm and (c) 800 nm.

of the PSCs. Figure 5 displays the total photo-generated carrier profiles (G_{tot}) of the three proposed architectures under AM1.5 G solar spectrum illumination. Maximum total photo-generated carrier (G_{tot}) in perovskite happens in front parts of the layer near the interface of ETL.

Coupling the optical results with the electrical module, we can achieve J-V curve of the PSC structures as the most important electrical characteristics of the solar cell. Figures 6(a) and (b) depict IPCE spectrum and J-V curve of the solar cells with planar, concave and trapezoidal architecture, respectively. The concavity height (C), the trapezius height (T_1) and short base (T_2) in this simulation, all are set at 50 nm. Looking at Figure 6(b), it is conspicuous that the best J-V curve belongs to the concave structure. Such result was expected due to the higher absorption of concave cell relative to two other structures (Figure 3). Short circuit current density (J_{sc}), Open-circuit voltage (V_{oc}), Fill Factor (FF) and Power

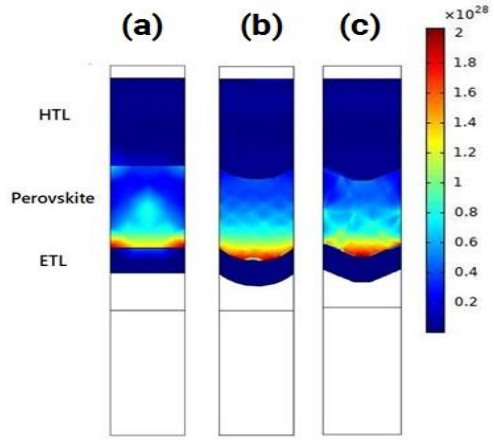

Figure 5. Total carrier photo-generation rate profiles (G_{tot}) in ETL, perovskite and HTL for (a) planar (b) concave and (c) trapezoidal structures over the wavelength range of 300-800 nm

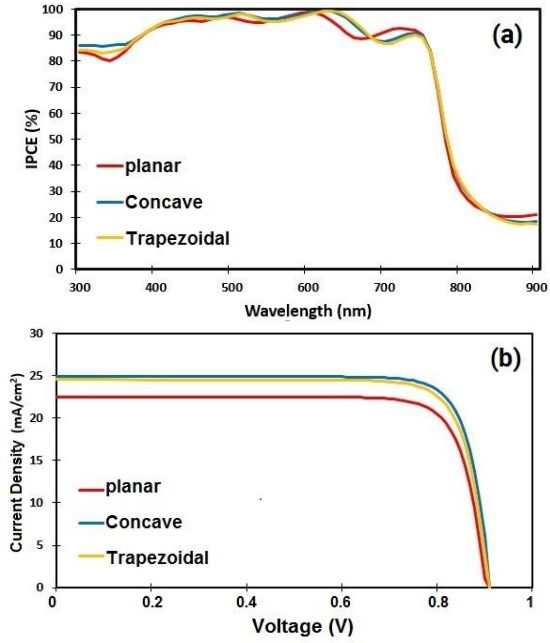

Figure 6. (a) IPCE and (b) Current Density-Voltage characteristics of the three proposed PSCs

Conversion Efficiency (η) values as important electrical results obtained from the J-V curve are listed in Table 2. As can be observed in Figure 6 and Table 2, the open-circuit voltage (V_{oc}) is almost the same for all types of simulated PSC devices. This can be attributed to the same materials, thicknesses and contacts that we used in all structures in our simulations. Despite that, short circuit current density (J_{sc}) for devices with nano-textured substrate witnesses a substantial increase compared to their planar counterpart. The utmost improvement in short circuit current density belongs to the concave

TABLE 2. The electrical performance results of the planar, concave and trapezoidal PSCs in this work and nanotubular and corrugated structures in previous works

Structure	J_{sc} (mA/cm^2)	V_{oc} (V)	FF (%)	PCE (%)
Planar	20.06	0.88	75	13.16
The proposed concave	25.7	0.9	80	18.5
The proposed trapezoidal	23.2	0.9	79.5	16.6
Nanotubular [17]	24.29	1	62.7	15.2
Corrugated contact [18]	23.4	0.93	77.1	17.5

structure with J_{sc}= 25.7 mA/cm^2 which shows 28 and 10% increase in comparison with the planar and trapezoidal structures, respectively. The fill factor of the planar structure rises from 75 to 80% for concave and 79.5% for trapezoidal structures. This increase can be related to the enhanced interface area which leads to smaller series resistances between perovskite and carrier transfer layers. Regarding power conversion efficiency, the highest efficiency still belongs to the concave PSCs with 18.5% and trapezoidal PSCs with 16.6% which shows a significant surge compared to the planar PSC with around 13.2% efficiency.

Lastly, we investigate the effects of the nanostructures height on the electrical performance of PSCs. Figure 7 shows the variation of the J_{sc}, V_{oc}, FF and PCE as a function of concavity and trapezius height (C and T_1). The highest J_{sc} happens at C=50 nm for concave PSC and T_1=70 nm for trapezoidal structure. V_{oc} does not change significantly with the nanostructures height. It was predictable since difference between quasi-fermi levels under the solar illumination mainly depends on the materials of PSC, and the impact of nanostructures height is negligible. For both structures, the highest FF belongs to the 50 nm nanostructures height. Regarding the PCE, the best efficiency occurs at 50 nm height for concave structure (C=50 nm), reaching 18.5% efficiency. In

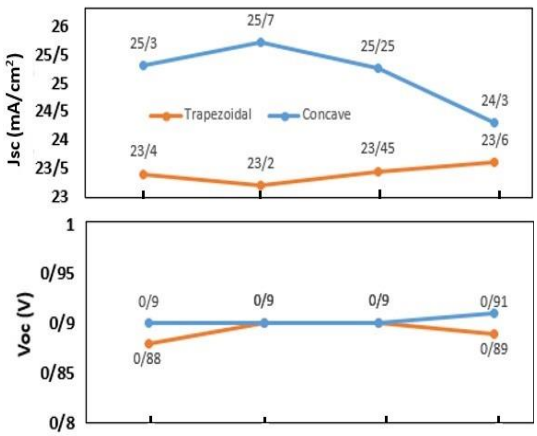

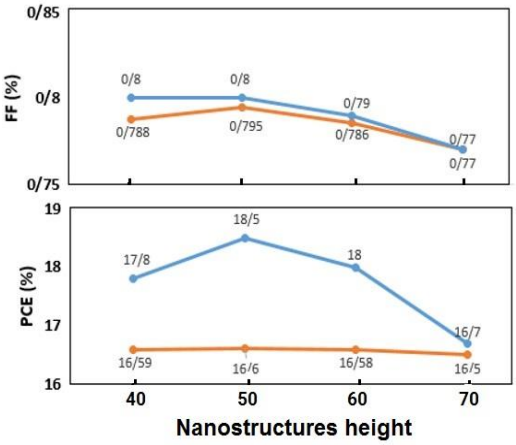

Figure 7. Variations of perovskite solar cell performance as a function of nanostructures height.

contrast to the concave structure, the PCE of trapezoidal PSC remains almost unchanged with the nanostructure height variations.

4. CONCLUSION

In this paper, the effect of using nano-textured substrates as light trapping architectures on improving the perovskite solar cells performance was investigated. Two different structures (concave and trapezoidal) of perovskite-based solar cells were designed, and different dimensions of the proposed structures were simulated to adopt the optimum values and enhance the overall efficiency. The analysis of the absorption in the active layer of the proposed structures normalized to the planar one over the wavelengths range of 300 to 800 nm demonstrated that the absorption enhances up to 32% in concave and 26% in trapezoidal structures at the wavelength of about 550 nm and at the height of 70 nm. In addition, we found that using concave and trapezoidal substrates can enhance the short-circuit current by around 28 and 15%, respectively. Accordingly, the power conversion efficiency was increased from 13.16% for planar PSC to 16.6% for trapezoidal, and 18.5% for concave structures at the height of 50 nm. It was shown that these improvements were related to the enhanced absorption, total carrier generation, and less series resistance in the proposed structures. It is thought that these achievements may open a new route for the fabrication of high efficiency perovskite solar cells through nano-textured substrates.

5. ACKNOWLEDGMENT

The authors acknowledge the funding support of Babol Noshirvani University of Technology, Iran through grant program No. BNUT/370557/99.

6. REFERENCES

1. Ke, W., Stoumpos, C.C., Zhu, M., Mao, L., Spanopoulos, I., Liu, J., Kontsevoi, O.Y., Chen, M., Sarma, D., Zhang, Y. and Wasielewski, M.R., "Enhanced photovoltaic performance and stability with a new type of hollow 3D perovskite {en} FASnI3." ***Science Advances,*** Vol. 3, No. 8, (2017), e1701293. doi: 10.1126/sciadv.1701293
2. Calvo, M. E., "Materials chemistry approaches to the control of the optical features of perovskite solar cells." ***Journal of Materials Chemistry A,*** Vol. *5*, No. 39, (2017), 20561-20578. doi: 10.1039/C7TA05666D
3. Fagiolari, L., and Federico, B., "Carbon-based materials for stable, cheaper and large-scale processable perovskite solar cells." ***Energy & Environmental Science,*** Vol. 12, No. 12, (2019), 3437-3472. doi: 10.1039/C9EE02115A.
4. Makableh, Y.F., Awad, I.A., Hassan, W. and Aljaiuossi, G., "Enhancement of the thermal properties of heterojunction perovskite solar cells by nanostructured contacts design." ***Solar Energy,*** Vol. 202, (2020), 204-209. doi: 10.1016/j.solener.2020.04.002
5. Wang, W., Winkler, M.T., Gunawan, O., Gokmen, T., Todorov, T.K., Zhu, Y. and Mitzi, D.B., "Device characteristics of CZTSSe thin-film solar cells with 12.6% efficiency." ***Advanced Energy Materials,*** Vol. 4, No. 7, (2014), 1301465. doi: 10.1002/aenm.201301465.
6. Khalate, S.A., Kate, R.S. and Deokate, R.J., "A review on energy economics and the recent research and development in energy and the Cu2ZnSnS4 (CZTS) solar cells: A focus towards efficiency." ***Solar Energy,*** Vol. 169, (2018), 616-633. doi: 10.1016/j.solener.2018.05.036.
7. Kojima, A., Teshima, K., Shirai, Y. and Miyasaka, T., "Organometal halide perovskites as visible-light sensitizers for photovoltaic cells." ***Journal of the American Chemical Society,*** Vol. 131, No. 17, (2009), 6050-6051. doi: 10.1021/ja809598r.
8. Zhang, F., Wang, Z., Zhu, H., Pellet, N., Luo, J., Yi, C., Liu, X., Liu, H., Wang, S., Li, X. and Xiao, Y., "Over 20% PCE perovskite solar cells with superior stability achieved by novel and low-cost hole-transporting materials." ***Nano Energy,*** Vol. 41, (2017), 469-475. doi: 10.1016/j.nanoen.2017.09.035.
9. Cahen, D., Zuo, C., Bolink, H.J., Han, H., Huang, J. and Ding, L., "Advances in perovskite solar cells." ***Advanced Science,*** Vol. 3, No. 7, (2016), 1500324. doi: 10.1002/advs.201500324.
10. Schulze, P.S., Bett, A.J., Winkler, K., Hinsch, A., Lee, S., Mastroianni, S., Mundt, L.E., Mundus, M., Würfel, U., Glunz, S.W. and Hermle, M., "Novel low-temperature process for perovskite solar cells with a mesoporous TiO_2 scaffold." ***ACS Applied Materials & Interfaces,*** Vol. 9, No. 36, (2017), 30567-30574. doi: 10.1021/acsami.7b05718.
11. Li, J. F., H. Y. Hao, J. B. Hao, L. Shi, J. J. Dong, H. Liu, and J. Xing. "Light trapping effect of textured FTO in perovskite solar cells." In IOP Conference Series: Materials Science and Engineering, Vol. 479, No. 1, 012046. IOP Publishing, (2019).
12. Saidaminov, M.I., Williams, K., Wei, M., Johnston, A., Quintero-Bermudez, R., Vafaie, M., Pina, J.M., Proppe, A.H., Hou, Y., Walters, G. and Kelley, S.O., "Multi-cation perovskites prevent carrier reflection from grain surfaces." ***Nature Materials,*** Vol. 19, No. 4, (2020), 412-418. doi: 10.1038/s41563-019-0602-2.
13. Tang, Z., Tress, W. and Inganäs, O., "Light trapping in thin film organic solar cells." ***Materials Today,*** Vol. 17, No. 8, (2014), 389-396. doi: 10.1016/j.mattod.2014.05.008.
14. Irandoost, R. and Soleimani-Amiri, S., "Design and analysis of high efficiency perovskite solar cell with ZnO nanorods and plasmonic nanoparticles." ***Optik,*** Vol. 202, (2020), 163598. doi: 10.1016/j.ijleo.2019.163598.

15. Abdelraouf, O.A., Abdelrahaman, M.I. and Allam, N.K., "Plasmonic scattering nanostructures for efficient light trapping in flat czts solar cells." In *Metamaterials XI,* Vol. 10227, p. 1022712**.** ***International Society for Optics and Photonics***, (2017), doi: 10.1117/12.2265249.
16. Adinolfi, V., Peng, W., Walters, G., Bakr, O.M. and Sargent, E.H., "The electrical and optical properties of organometal halide perovskites relevant to optoelectronic performance." ***Advanced Materials,*** Vol. 30, No. 1, (2018), 1700764. doi: 10.1002/adma.201700764.
17. Abdelraouf, O.A. and Allam, N.K., "Towards nanostructured perovskite solar cells with enhanced efficiency: Coupled optical and electrical modeling." ***Solar Energy,*** Vol. 137, (2016), 364-370. doi: 10.1016/j.solener.2016.08.039.
18. Zandi, S. and Razaghi, M., "Finite element simulation of perovskite solar cell: A study on efficiency improvement based on structural and material modification." ***Solar Energy,*** Vol. 179, (2019), 298-306. doi: 10.1016/j.solener.2018.12.032.
19. Wenger, S., Schmid, M., Rothenberger, G., Gentsch, A., Gratzel, M. and Schumacher, J.O., "Coupled optical and electronic modeling of dye-sensitized solar cells for steady-state parameter extraction." ***The Journal of Physical Chemistry C,*** Vol. 115, No. 20, (2011), 10218-10229. doi: 10.1021/jp111565q.
20. Schöche, S., Hong, N., Khorasaninejad, M., Ambrosio, A., Orabona, E., Maddalena, P. and Capasso, F., "Optical properties of graphene oxide and reduced graphene oxide determined by spectroscopic ellipsometry." ***Applied Surface Science,*** Vol. 421, (2017), 778-782. doi: 10.1016/j.apsusc.2017.01.035.
21. Ball, J.M., Stranks, S.D., Hörantner, M.T., Hüttner, S., Zhang, W., Crossland, E.J., Ramirez, I., Riede, M., Johnston, M.B., Friend, R.H. and Snaith, H.J., "Optical properties and limiting photocurrent of thin-film perovskite solar cells." ***Energy & Environmental Science,*** Vol. 8, No. 2, (2015), 602-609. doi: 10.1039/C4EE03224A.
22. Deceglie, M.G., Ferry, V.E., Alivisatos, A.P. and Atwater, H.A., "Design of nanostructured solar cells using coupled optical and electrical modeling**."** ***Nano Letters,*** Vol. 12, No. 6, (2012), 2894-2900. doi: 10.1021/nl300483y.
23. Barrit, D., Cheng, P., Tang, M.C., Wang, K., Dang, H., Smilgies, D.M., Liu, S., Anthopoulos, T.D., Zhao, K. and Amassian, A., "Impact of the Solvation State of Lead Iodide on Its Two-Step Conversion to MAPbI3: An In Situ Investigation." ***Advanced Functional Materials,*** Vol. 29, No. 47, (2019), 1807544. doi: 10.1002/adfm.201807544.

Persian Abstract

چکیده

در سال های اخیر ، استفاده از سلول های خورشیدی ترکیبی آلی غیر معدنی پروسکایت تحت طراحی پیشرفته و به دام اندازی نور، توجه زیادی را به خود جلب کرده است. در این مقاله، برای بررسی ویژگی های نوری و الکتریکی در سلول های خورشیدی پروسکایت با نانو ساختارها، از روش المان محدود سه بعدی استفاده شده است. با استفاده از لایه های اکسید قلع دوپینگ شده با فلور نانو بافت (FTO) ، ما دو معماری مختلف را پیشنهاد می‌کنیم که می‌توانند نور را در ابعاد نانومتر به دام بیندازند. دو ساختار پیشنهادی یعنی ساختارهای مقعر و ذوزنقه ای به منظور بررسی تأثیرات استفاده از لایه های نانوساختار بر عملکرد سلول های خورشیدی پروسکایت با ساختار مسطح مقایسه می‌شوند. تجزیه و تحلیل نوری نشان می‌دهد که استفاده از ساختارهای مقعر و ذوزنقه‌ای بهینه می‌تواند جذب نور را در طول موج 550 نانومتر به ترتیب تا 32 و 26 درصد افزایش دهد. شبیه سازی های الکتریکی نشان داده اند که علاوه بر افزایش تولید حامل های کل ، حامل های تولید شده را می توان به طور موثر در نانو ساختار پیشنهادی بدست آورد. بر این اساس ، جریان اتصال کوتاه از 20 میلی آمپر برای ساختار مسطح به 25.7 میلی آمپر برای مقعر و 23.2 میلی آمپر برای سلول خورشیدی پروسکایت با معماری ذوزنقه ای افزایش یافته است. پس از تجزیه و تحلیل ارتفاعات مختلف و با اتخاذ مقادیر بهینه ، بازده تبدیل نیرو برای سلول های خورشیدی پروسکایت با ساختارهای مقعر و ذوزنقه نسبت به ساختار مسطح 5.5٪ و 3.5٪ افزایش قابل ملاحظه‌ای داشته است. این پیشرفت های قابل توجه که توسط مدل نوری و الکتریکی همراه نانو ساختار مورد تجزیه و تحلیل قرار گرفته است ، می‌تواند راه را برای مطالعات بیشتر برای ساخت سلول های خورشیدی پروسکایت با بازدهی بالا با لایه های نانو ساختار به عنوان روش به دام اندازی نور فراهم کند.